IEEE Access
Multidisciplinary ⋮ Rapid Review ⋮ Open Access Journal

Received April 20, 2022, accepted May 13, 2022, date of publication June 3, 2022, date of current version June 13, 2022.

Digital Object Identifier 10.1109/ACCESS.2022.3180048

Compact Multiband Reconfigurable MIMO Antenna for Sub- 6GHz 5G Mobile Terminal

SURENTIRAN PADMANATHAN[1], (Member, IEEE), AZREMI ABDULLAH AL-HADI[1], (Senior Member, IEEE), AHMED MOHAMED ELSHIRKASI[1], SAMIR SALEM AL-BAWRI[2,3], (Member, IEEE), MOHAMMAD TARIQUL ISLAM[4], (Senior Member, IEEE), THENNARASAN SABAPATHY[1], (Member, IEEE), MUZAMMIL JUSOH[1], (Senior Member, IEEE), PRAYOOT AKKARAEKTHALIN[5], (Senior Member, IEEE), AND PING JACK SOH[1,6], (Senior Member, IEEE)

[1]Advance Communication Engineering (ACE) Centre of Excellence, Faculty of Electronic Engineering Technology, Universiti Malaysia Perlis, Kangar, Perlis 01000, Malaysia
[2]Space Science Centre, Climate Change Institute, Universiti Kebangsaan Malaysia (UKM), Bangi 43600, Malaysia
[3]Department of Electronics and Communication Engineering, Faculty of Engineering, Hadhramout University, Al-Mukalla, Yemen
[4]Department of Electrical, Electronics and System Engineering, Faculty of Electric and Built Environment, Universiti Kebangsaan Malaysia (UKM), Bangi, Selangor 43600, Malaysia
[5]Department of Electrical and Computer Engineering, Faculty of Engineering, King Mongkut's University of Technology North Bangkok (KMUTNB), Wongsawang, Bangsue, Bangkok 10800, Thailand
[6]Centre for Wireless Communications (CWC), University of Oulu, 90570 Oulu, Finland

Corresponding author: Azremi Abdullah Al-Hadi (azremi@unimap.edu.my)

This work was supported in part by the Ministry of Education, Malaysia; in part by the National Science, Research and Innovation Fund (NSRF); and in part by the King Mongkut's University of Technology North Bangkok under Contract KMUTNB-FF-65-21. The work of Ping Jack Soh was supported by the Academy of Finland Genesis Flagship under Grant 318927.

ABSTRACT In this paper, the design of a multiband multiple-input multiple-output (MIMO) antenna with frequency and radiation pattern reconfiguration capability in the 5G sub-6 GHz band is presented. Frequency and radiation pattern reconfiguration are enabled on the antenna consisting of two planar inverted-F antenna (PIFA) elements using PIN diodes and DC biasing circuits. At the reflection coefficients of less than −6 dB, both PIFA element 1 and PIFA element 2 achieves triband with bandwidth from 220 MHz to 2330 MHz, ranging from 0.8 GHz to 6 GHz, covering cellular bands for GSM, UMTS, LTE and 5G-NR bands. Moreover, high isolation of at least −10 dB and envelope correlation coefficient with less than 0.3 between ports ensures satisfactory MIMO diversity performance. PIFA elements 1 and 2 have achieved main lobe gain ranging from 1.06 dB to 2.97 dB at their respective resonant frequencies with total efficiencies ranging from 46.2% to 74.5% achieved within the operating bandwidth. This enables a calculated channel capacity of 9.45 to 10.5 bit/s/Hz for PIFA element 1 and 9.56 to 10.23 bit/s/Hz for PIFA element 2, respectively. The percentage of channel capacity achieved over IID capacity for both PIFA elements ranges from 73.71% to 92.8%. Simulated antenna performance parameters agreed well with measurements, and potentially enables reliable and consistent data throughput for 5G mobile terminals.

INDEX TERMS 5G, MIMO antennas, mobile terminals, multiband antennas, reconfigurable antennas.

I. INTRODUCTION

The success of Fourth Generation (4G) long term evolution (LTE) via the adoption of multiple input multiple output (MIMO) technology in the previous decade has resulted a great enhancement in mobile communication technology. As a result, the use of smart mobile phones with various flagship features has significantly increased in recent years. Consequently, the demand for high data rate with improved reliability in mobile phones has also emerged as critical requirement. These demands include high quality video calls, stream high definition (HD) videos and play HD online games [1], [2]. Furthermore, the recent COVID-19 pandemic highlighted the importance of high throughput network connections for remote working. It is foreseen that the release of Fifth Generation-New Radio (5G-NR) sub-6 GHz spectrum

The associate editor coordinating the review of this manuscript and approving it for publication was Zesong Fei.

[3], [4] using MIMO technology will further advance mobile communications towards 5G [5]. This technology triggered research into MIMO antennas, as this will enable wireless devices with such features in 5G to operate with excellent system throughput and intensive data processing capability.

As a result, antennas are required to have multiband coverage or frequency tuning feature to adapt newly released frequency bands such as 5G-NR together with other sub-6 GHz bands. In addition, the implementation of microcell architecture in 5G requires the support of high gain and directive antennas to mitigate multipath fading and pathloss in mobile terminals. Antenna miniaturization also become increasingly critical in fulfilling the requirements of closely packed antenna arrangements in 5G MIMO mobile terminals [6], [7]. Making the compact antenna structures in MIMO mobile terminals multiband and reconfigurable is an appealing feature for 5G technology [8], [9]. Reconfigurable antenna is an active antenna which has the ability to reconfigure the antenna parameters such as radiation pattern, resonant frequency and polarization. Frequency reconfigurable antenna has the flexibility to tune the resonant frequency over a wide range of frequency band, regardless of the antenna's structural dimension [10]. Radiation pattern reconfigurable antenna has the advantage to mitigate the multipath loss in rich scattering environment by reconfiguring the antenna's radiation pattern beam towards the noise-null direction [11]. The research work presented in this paper advances this concept a step further by proposing a compact multiband reconfigurable MIMO antenna with frequency and radiation pattern reconfiguration operating in the sub-6 GHz band for mobile terminals. This two-port mobile terminal antenna is designed by integrating two planar inverted-F antennas (PIFA1 and PIFA2) in a compact form ($0.06\ \lambda_0 \times 0.04\ \lambda_0 \times 0.021\ \lambda_0$ and $0.12\ \lambda_0 \times 0.05\ \lambda_0 \times 0.05\ \lambda_0$ for PIFA1 and PIFA2, respectively) at each port. PIFA is adapted in this work since it is widely used as an internal antenna in wireless communication systems due to its wide operating band, simple structure, good radiation patterns, and ease of integration with other active devices. The placement of two PIFA elements at each port is intended to make one of them a parasitic element when another element is activated. As a result, resonance at lower frequency band (below 1 GHz) and multiple resonances can be achieved through coupling effect. In addition, frequency reconfiguration is also enabled when the activation is switched between PIFA 1 and PIFA 2, as both PIFA elements resonates at different frequency bands. On the other hand, due to the coupling effect, both PIFA elements also achieves common -6 dB bandwidth, allowing for the observation of radiation pattern reconfiguration at the common frequency bands, as PIFA 1 and PIFA 2 are positioned non-identically.

Previously, the proposed MIMO mobile terminal antennas are either unable to provide coverage for 5G-NR band [12]–[15], or without simultaneous multiband operation and/or reconfiguration capabilities [16]–[18]. The proposed antenna design in [12] consists of eight elements on a single substrate board. Frequency reconfigurability is only achieved between 1.6 to 2.48 GHz using a varactor diode by varying the capacitive reactance. The antenna design in [13] consist of dual-band PIFA for the LTE-M (700∼900 MHz) and LTE-2500 bands, with the LTE-M band's PIFA being frequency reconfigurable. This design however has limited cellular band coverage while consuming broader space with large design structure. The 2 MIMO antenna system described in [14] uses the smartphone's metallic frame and a stub network to execute frequency reconfiguration across the entire LTE spectrum, which spans 699–960 MHz (lower frequency spectrum) and 1710–2690 MHz (higher frequency spectrum). Similarly, the proposed antenna in [15] has four monopole slots, two of which are long monopole slots with two PIN diodes inserted. When these two PIN diodes are turned OFF and ON, two long monopole slots and four short monopoles slots are activated respectively, producing the desired lower-band (824–960 MHz) and upper-band (1710–2690 MHz) frequency coverage. As can be seen, both these antennas only cover a limited number of cellular bands and are incapable of covering the 5G-NR spectrum. The proposed antenna in [16] is only capable to perform radiation pattern reconfiguration at 5 GHz single band. Two centro-symmetrically distributed antenna elements and radiation structures are used in a reconfigurable full-metal-rimmed MIMO antenna reported in [17]. This hepta-band MIMO antenna are only able to cover lower GSM850/900 bands and higher GSM1800/1900/UMTS/LTE2300/2500 bands using a reconfigurable technique. [18] proposes a MIMO antenna with two symmetrical PIFAs for dual-band tunability between 0.8 and 0.98 GHz in the lower band and 1.65 to 2.2 GHz in the higher band. The suggested antenna allows for independent frequency tuning while avoiding interference with the frequency bands. The multiband MIMO antennas in literature [19]–[21] are not frequency reconfigurable, potentially limiting their cellular band coverage and adaptability to the new 5G-NR bands. There have been no reported MIMO antennas with multiband operation as well as simultaneous frequency and radiation pattern reconfiguration capabilities in the same structure. Furthermore, it is evident that these antennas lack a wider tuning range to cover multiple cellular bands including 5G-NR. To the best of our knowledge, this is the first of such antenna to be reported in open literature which has been constructed in compact form to produce coverage for multiple cellular bands including 5G-NR band, and perform frequency reconfiguration and radiation pattern reconfiguration together.

II. ANTENNA SYSTEM DESIGN

A. DESIGN METHOD

Fig. 1 shows the proposed antenna modeled in Computer Simulation Technology (CST) software. Each antenna consists of two PIFA elements (PIFA 1 and PIFA 2). To form the MIMO antenna, two sets of these antennas are each placed at the top left and right of a rectangular (120 mm × 60 mm × 1.575 mm) FR4 substrate, as shown in Fig. 1(a).

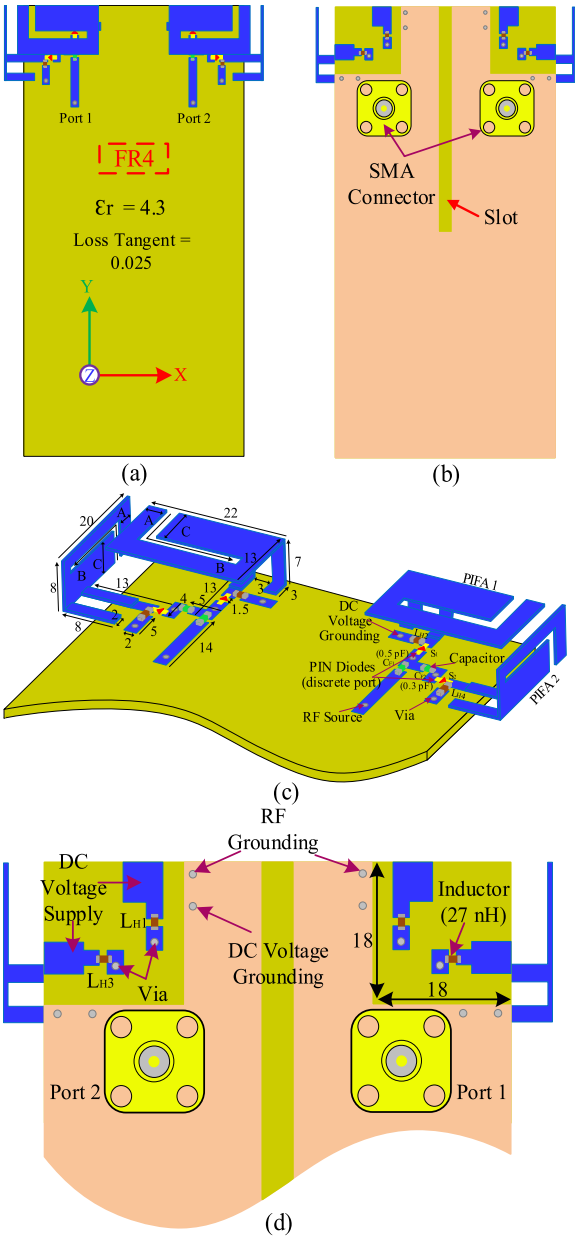

FIGURE 1. Geometry of the proposed MIMO antenna. (a) front view (terminal) (b) rear view (terminal) (c) perspective view (PIFA elements) (d) rear view (PIFA elements). All dimensions are in millimeter (mm).

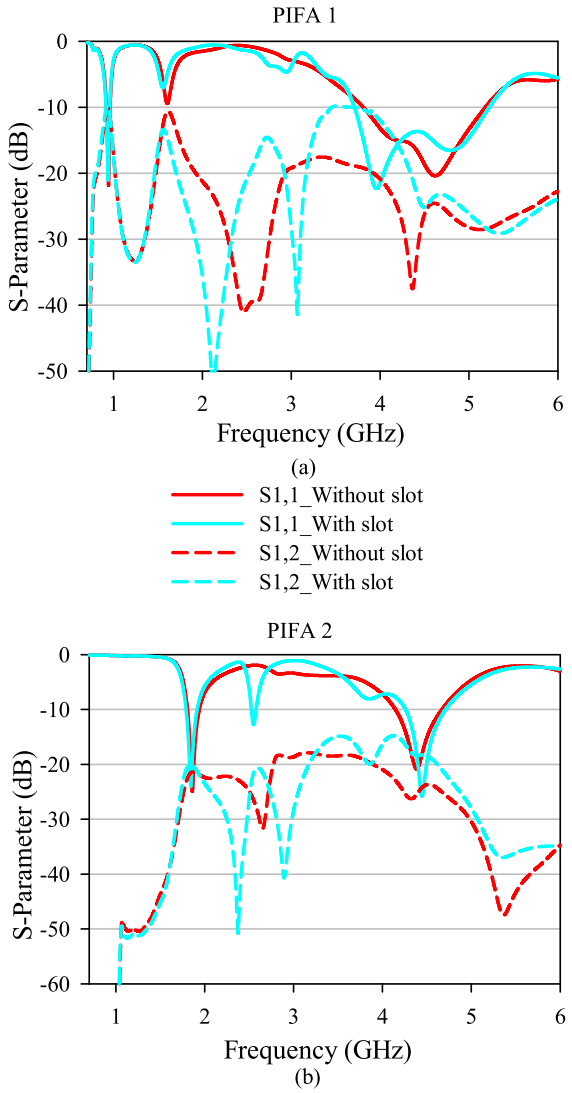

FIGURE 2. The effect of the L-Shaped slot on the S-Parameter results of (a) PIFA 1 and (b) PIFA 2.

An identically sized copper ground plane with a thickness of 0.035 mm is introduced on the bottom layer of the substrate, as depicted in Fig. 1(b). A 30 mm × 4 mm slot is integrated on this ground plane and centered between the two antennas to reduce mutual coupling between them.

The detailed dimensions of the PIFA elements are shown in Fig. 1 (c). Two PIN diodes (BAR50-02V), S_1 and S_2, and a DC biasing circuit (with $C_{F1} = 0.5$ pF and $C_{F2} = 0.3$ pF, and 27 nH for all inductors) is used on each antenna (each port) to separately activate PIFA element 1 and 2 to enable frequency and radiation pattern reconfiguration. From both ports, either PIFA 1 or PIFA 2 are activated/deactivated simultaneously using the respective PIN diode (S_1 and S_2).

In this way, the activated PIFA element acts as the *driven element*, whereas the inactive PIFA element couples to the *driven element* as the *parasitic element*. Upon the activation of a PIFA element (either PIFA 1 or PIFA 2), the RF current from the *driven element* couples strongly with the *parasitic element*, increasing the electrical length. This lengthens its wavelength, λ, thus lowering its operating band. As a result, resonance at lower frequency bands (below 1 GHz). Moreover, the coupling effect also induces these PIFA elements to produce multiple resonances. Besides this, in order to perform frequency reconfiguration, PIFA 1 and PIFA 2 should be able to produce separate frequency bands when activated, respectively. We discovered that the size of the PIFA radiator (patch) and the length of the feed strips play an important role in achieving the desired resonant frequency for each PIFA elements. Therefore, parameter optimization is conducted to obtain unidentical length, L, and width, W, of the patch in both PIFA elements 1 and 2. Moreover, the lengths of the feed strips for PIFA element 1 ($l_{f1} = 34$ mm) and

PIFA element 2 ($l_{f2} = 36$ mm) are constructed with different dimensions to enable frequency reconfiguration.

On the other hand, the reconfiguration of the radiation pattern is possible to be observed in our proposed design, as these two PIFA elements achieves a common −6 dB bandwidth due to the coupling effect. As both PIFA elements are placed in orthogonal orientation, the beams are directed towards separate directions, allowing beam reconfiguration when activated/deactivated via the PIN diodes. The DC voltage supply and grounding terminals are mounted at the bottom of the substrate with ground clearance of 18 mm × 18 mm, as shown in Fig. 1(d). Followingly, we have conducted a study on the effect of inserting the L-shaped slots on the radiators of PIFA elements. From Fig. 1(c), we can see that the L-shaped slot comprises three dimensions, *A*, *B* and *C*. Distance *A* is the separation length between the edge of the patch and the opening of the slot, while distance *B* is the total length of the slot. On the other hand, distance *C* is the dimension between the edge of the patch and the horizontal part of slot. Parameter sweeps were performed to tune dimensions *A*, *B* and *C* for optimal reflection coefficients. It can be seen that the slot has a significant impact on the PIFA elements' ability to achieve wider bandwidths with good impedance when compared to the PIFA element without a slot, as illustrated in Fig. 2.

B. BIASING CIRCUITRY

The integration of PIN diodes in reconfigurable antenna design is a critical procedure that necessitates the use of a Direct Current (DC) biasing circuit. The overall schematic diagram with two sets of PIN diodes (S_1 & S_2) and DC biasing circuits for port 1 is illustrated in Fig. 3. Port 2 has the similar setup as port 1, since both ports are symmetric to each other. From the figure, it can be noticed that the path of Radio Frequency (RF) current is controlled by the PIN diode and DC biasing circuit to enable the radiation through the respective PIFA element. The connection between the PIFA element and RF source is allowed when the DC voltage is fed through the via to forward bias the PIN diode, thus activating it. As a result, the RF current flows through the microstrip line and radiate through the patch of PIFA element. On the other hand, no voltage supply or zero voltage is fed to reverse bias the PIN diode, thus deactivating it to disable the radiation. The inductors/RF chokes (L_H) are connected to the PIN diode at the positive and grounding terminals of the DC voltage to prevent the RF current from entering the DC biasing line. Capacitors (C_F), on the other hand, are placed on the microstrip prior to the PIN diode to suppress the DC voltage and allow the RF current to flow towards the respective PIFA element.

Integrating real PIN diode and lumped components on the fabricated antenna may affect the measured results. Therefore, to reduce the variation between simulated and measured results, we acquired from the manufacturer a touchstone block (BAR50-02V) made of s2p files containing s-parameter information for ON and OFF conditions and used it in simulation. Similarly, the inductors and capacitors

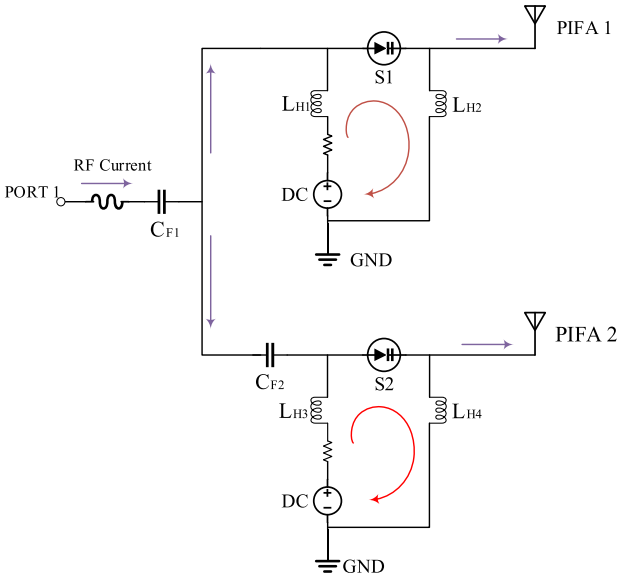

FIGURE 3. The schematic diagram of DC biasing circuit for PIFA element 1 and PIFA element 2 at port 1.

utilized in our design during simulation were obtained from the manufacturer. Nevertheless, in the practical scenario, the PIN diode has different isolation loss according to the amount of capacitance it holds during OFF state. Furthermore, the diode will be acting as RL_H series circuit and RC_F shunt circuit, respectively at ON and OFF condition. Hence, the placement of biasing circuit that comprises of capacitors and inductors, and the interference from the DC wires may affect the capacitance of the diode which leads to the variation in the measured results. Moreover, the fringing effect of the transmission line also may alter the capacitance of the diode, influencing the measured results. The switching configuration of the antenna is tabulated in Table 1. When the PIN diode is set to mode 1, PIFA 1 from port 1 and 2 will be activated as *driven element*, allowing the RF current to radiate. Similarly, PIFA 2 from port 1 and 2 becomes *driven element* when the PIN diode is set to mode 2.

III. RESULTS AND DISCUSSION

A prototype of the proposed antenna consist of PIN diodes and lumped component was fabricated and measured to validate the simulation results, as shown in Fig. 4. Activation of the desired PIN diode (and consequently the desired PIFA element) is controlled by the switching control network, as shown in Fig. 4 (c). Measurements were performed in a Satimo Starlab anechoic chamber.

A. S-PARAMETER AND RADIATION PATTERN RESULTS

Fig. 5 shows the simulated and measured reflection coefficients of the two-port MIMO antenna. The S-Parameter (S_{11} and S_{22} or S_{21} and S_{12}) results obtained from port 1 and 2 are identical to each other as similar PIFA elements are activated concurrently at both ports. It is observed that measurements results are comparable with simulations. PIFA elements (1 and 2) from both ports operate in three bands

TABLE 1. The switching configuration for PIFA element 1 and PIFA element 2.

Port	PIN Diode configuration	PIFA Element	Connected Switch	Switch's State	Status
Port 1	Mode 1	PIFA 1	S1	ON	Radiator
		PIFA 2	S2	OFF	Parasitic
	Mode 2	PIFA 1	S1	OFF	Parasitic
		PIFA 2	S2	ON	Radiator
Port 2	Mode 1	PIFA 1	S1	ON	Radiator
		PIFA 2	S2	OFF	Parasitic
	Mode 2	PIFA 1	S1	OFF	Parasitic
		PIFA 2	S2	ON	Radiator

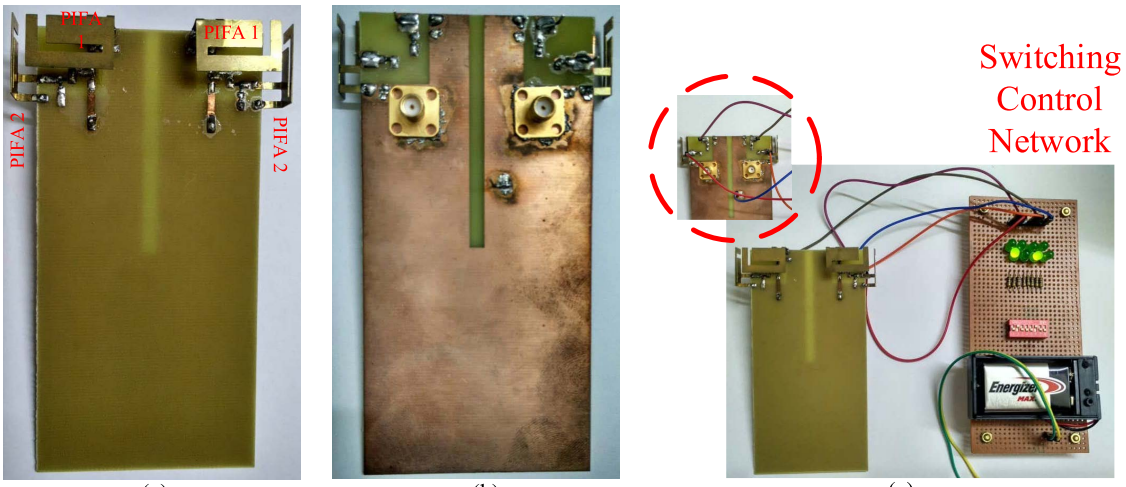

FIGURE 4. Fabricated MIMO antenna with BAR50-02V PIN diode and lumped components (a) Front view (b) Rear view and (c) Switching control network which used to control the activation of the desired PIN diode.

with at least $S_{11}/S_{22} < -6$ dB to cover the standard cellular frequencies in Table 2. When PIFA element 1 is activated as *driven element* (mode 1), it obtains the first resonant frequency at 0.94 GHz with the bandwidth of 260 MHz. In addition, it achieved the second and third resonant frequencies at 3.95 GHz and 4.75 GHz, respectively with a wider bandwidth of 2330 MHz together. When PIFA element 2 is activated as *driven element* (mode 2), it realizes triple resonant frequencies at 1.85 GHz, 2.55 GHz and 4.45 GHz with the bandwidth of 510 MHz, 220 MHz and 2000 MHz, respectively. As for the transmission coefficient result, S_{21} and S_{12}, mutual coupling of less than – 10 dB and has been achieved between port 1 and 2, at their respective resonances. The operating bandwidths of PIFA element 1 and PIFA element 2 are non-identical, as shown in Fig. 5 (a) and (b). Thus, besides being triband/multiband, their combined operation enables frequency reconfiguration when the PIN diodes are activated/deactivated between PIFA element 1 and 2.

Next, simulated and measured radiation patterns of PIFA element 1 (at 0.94, 3.95 and 4.75 GHz) and PIFA element 2 (at 1.85, 2.55 and 4.45 GHz) are shown in Fig. 6 and Fig. 7, respectively. These radiation pattern results of both PIFA elements that were obtained at respective resonant frequencies are illustrated at both xz-plane and xy-plane. We noticed that the PIFA element 1 has achieved maximum main lobe gain of 1.06 dB, 1.23 dB and 2.37 dB for the resonant frequencies of 0.94 GHz, 3.95 GHz and 4.75 GHz, respectively in xy-plane. On the other hand, PIFA element 2 has achieved maximum

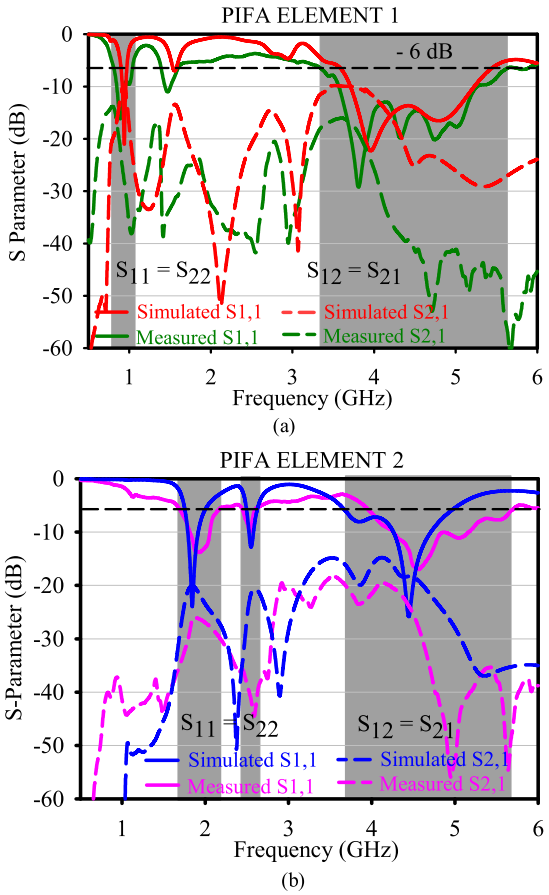

FIGURE 5. Simulated and measured S-parameters for (a) PIFA element 1 and (b) PIFA element 2.

main lobe gain of 2.97 dB, 1.5 dB and 1.87 dB for the resonant frequencies of 1.85 GHz, 2.55 GHz and 4.45 GHz, respectively in xy-plane. In addition to achieving multiple resonant frequencies and frequency reconfiguration, our proposed antenna which accommodates dual PIFA elements within a single port allows the antenna to reconfigure the beam. The achievement of identical resonant frequency or common −6 dB bandwidth between both PIFA elements is essential to monitor the reconfiguration of the radiation pattern. The intended coupling between the activated/deactivated PIFA elements within the same port enabled them to operate with identical resonant frequencies. Fig. 8 illustrates the achieved common −6 dB bandwidth of 1750 MHz by PIFA element 1 and PIFA element 2 from 3.95 GHz to 5.7 GHz. As a result, beam reconfiguration is enabled when the two orthogonally directed PIFA elements are activated in sequence. It can be noticed that both PIFA elements has achieved the radiation pattern reconfiguration at 4.5 GHz when the PIFA elements are activated in sequence.

Fig. 9 and 10 shows the two-dimensional and three-dimensional radiation pattern results obtained at the identical resonant frequency of 4.5 GHz. It can be seen from these figures that the radiation pattern undergoes certain degree of beam reconfiguration when the PIN diode switch activation is configured between PIFA element 1 and PIFA element 2.

TABLE 2. Cellular frequency bands covered by PIFA element 1 and 2.

Elements	PIFA 1	PIFA 2	Resonant Frequency (GHz)	Bandwidth (MHz)	Cellular Bands
PIFA Element Status	**Radiator**	Parasitic	0.94	260	GSM, UMTS, LTE, 5G-NR
			3.95	2330	UMTS, LTE, 5G-NR
			4.75		
	Parasitic	**Radiator**	1.85	510	GSM, UMTS, LTE, 5G-NR
			2.55	220	UMTS, LTE, 5G-NR
			4.45	2000	LTE, 5G-NR

Table 3 details the reconfigured radiation pattern of PIFA elements 1 and 2 at the identical resonant frequency of 4.5 GHz. From the table, it can be observed that the main lobe direction of PIFA element 1 and PIFA element 2 monitored at port 1 is directed towards 155° and 232° in the xy-plane, respectively. On the other hand, the main lobe direction of PIFA element 1 and PIFA element 2 observed at port 2 is pointing towards 25° and 308° in the xy-plane, respectively. As a result, we can conclude that the proposed antenna can reconfigure the radiation pattern in at least four different directions at the identical resonant frequency. Next, the simulated and measured total efficiency of PIFA element 1 and 2 is shown in Figure 11. PIFA element 1 has achieved simulated total efficiency of 59%, 76.4% and 82.24% at 0.94 GHz, 3.95 GHz and 4.75 GHz, respectively. The measured total efficiency of PIFA element 1 obtained at 0.94 GHz, 3.95 GHz and 4.75 GHz are 46.2%, 73.9% and 74.5%, respectively. On the other hand, PIFA element 2 has achieved simulated total efficiency of 78.7%, 57.7% and 79.6% at 1.85 GHz, 2.55 GHz and 4.45 GHz, respectively. The measured total efficiency for PIFA element 2 is 55.2%, 52.40% and 65.07% at 1.85 GHz, 2.55 GHz, and 4.45 GHz, respectively. It can be seen that all measured total efficiencies are slightly lower compared to calculated values due to the non-idealities of the actual PIN diodes and lumped components. Nevertheless, these values are still good and acceptable at deeply matched measured frequency points.

B. MIMO PERFORMANCES

The MIMO performance metrics of this antenna are evaluated in terms of envelope correlation coefficient (ECC) and

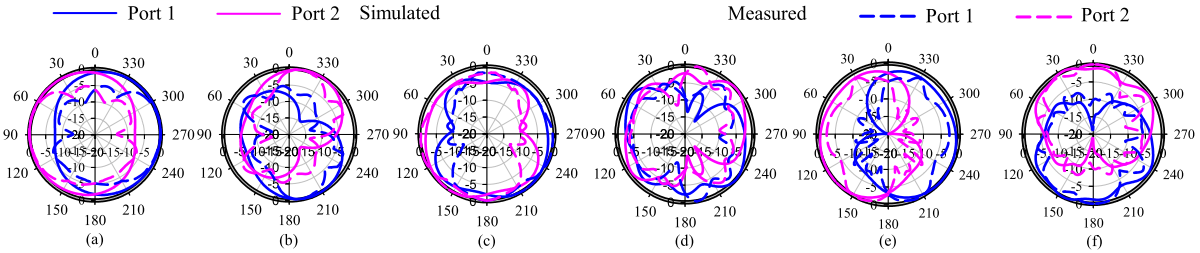

FIGURE 6. Simulated and measured radiation patterns of PIFA element 1 in the: (a) *xz*-plane and (b) *xy*-plane at 0.94 GHz; (c) *xz*-plane and (d) *xy*-plane at 3.95 GHz; and (e) *xz*-plane and (f) *xy*-plane at 4.75 GHz.

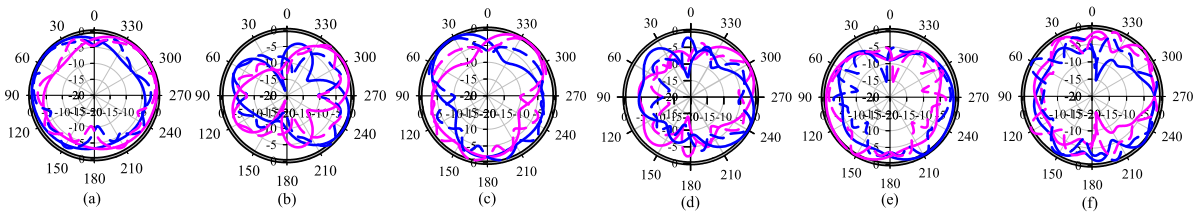

FIGURE 7. Simulated and measured radiation patterns of PIFA element 2 in the: (a) *xz*-plane and (b) *xy*-plane at 1.85 GHz; (c) *xz*-plane and (d) *xy*-plane at 2.55 GHz; and (e) *xz*-plane and (f) *xy*-plane at 4.45 GHz.

channel capacity [22]. The Fig. 12 shows the simulated and calculated ECC for both PIFA elements within their −6 dB bandwidths. It can be noticed that the ECC values of lesser than 0.26 and 0.08, respectively, is seen across the operating bands of PIFA 1 and PIFA 2, respectively. This shows that the main lobes of the PIFA elements from each port is uncorrelated, mainly due to the large distance between the two ports enabled by compact PIFA elements.

Followingly, the simulated and calculated channel capacity for PIFA element 1 and PIFA element 2 is depicted in Fig. 13. This is based on a 2 × 2 independent and identically distributed (IID) channel capacity calculated at a Signal to Noise Ratio (SNR) of 20 dB. The IID ergodic channel capacity (c_{IID}) for 2 × 2 MIMO system is 11.3 bit/s/Hz. From the figure, it can be noticed that PIFA element 1 has achieved the maximum simulated ergodic channel capacity, (c_{AUT}) of 9.86 bit/s/Hz, 10.56 bit/s/Hz and 10.77 bit/s/Hz at 0.94 GHz, 3.95 GHz and 4.75 GHz, respectively. The calculated maximum channel capacity achieved by PIFA element 1 are 9.45 bit/s/Hz, 10.47 bit/s/Hz and 10.5 bit/s/Hz at 0.94 GHz, 3.95 GHz, and 4.75 GHz, respectively. On the other hand, PIFA element 2 achieves the maximum simulated ergodic channel capacity, (c_{AUT}) of 10.63 bit/s/Hz, 9.84 bit/s/Hz and 10.68 bit/s/Hz, at the resonant frequencies of 1.85 GHz, 2.55 GHz and 4.45 GHz, respectively. The calculated maximum channel capacity achieved by PIFA element 2 are 9.72 bit/s/Hz, 9.56 bit/s/Hz and 10.23 bit/s/Hz, at 1.85 GHz, 2.55 GHz, and 4.45 GHz, respectively. Next, a comparison study between antenna element's ergodic channel capacity, (c_{AUT}) and the IID capacity, (c_{IID}) were evaluated in percentage. In simulation, PIFA element 1 achieved 86.7%, 93.45%, and 95.3% of the IID capacity at 0.94 GHz, 3.95 GHz, and 4.75 GHz, respectively.

In terms of measurement, PIFA element 1 achieved 83.6%, 92.6%, and 92.8% of the IID capacity at 0.94 GHz, 3.95 GHz, and 4.75 GHz, respectively. At 1.85 GHz, 2.55 GHz and 4.45 GHz, PIFA element 2 achieved 94.07%, 87.07%, and

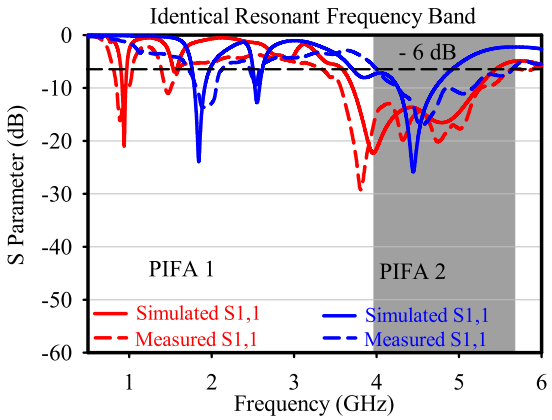

FIGURE 8. Identical resonant frequency band between PIFA element 1 and PIFA element 2.

94.51% of the IID capacity, respectively in terms of simulation. In measurement, PIFA element 2 achieved 86.1%, 84.6%, and 90.53% of the IID capacity at 1.85 GHz, 2.55 GHz and 4.45 GHz, respectively. Overall, the percentage range from minimum to maximum calculated channel capacity over the IID capacity is from 73.89% to 92.8% (for PIFA element 1) and 73.71% to 90.53% (for PIFA element 2). From the figure, it can be seen that both PIFA elements obtains the highest percentage (close to IID capacity) of the ergodic capacity (c_{AUT}) at higher frequency bands.

The proposed antenna is compared with other related literature in Table 4. The overall comparison study is organized based on the criteria such as type of antenna, antenna volume size, bandwidth, cellular band coverage, calculated efficiency, ECC and channel capacity. From the table, it can be noticed that there are no reported MIMO antennas exhibiting a multiband operation and simultaneous frequency and radiation pattern reconfiguration capabilities in the same structure. Despite being fabricated on a larger substrate than the proposed antenna, these antennas have a drawback in terms of space utilization due to constrained cellular band coverage.

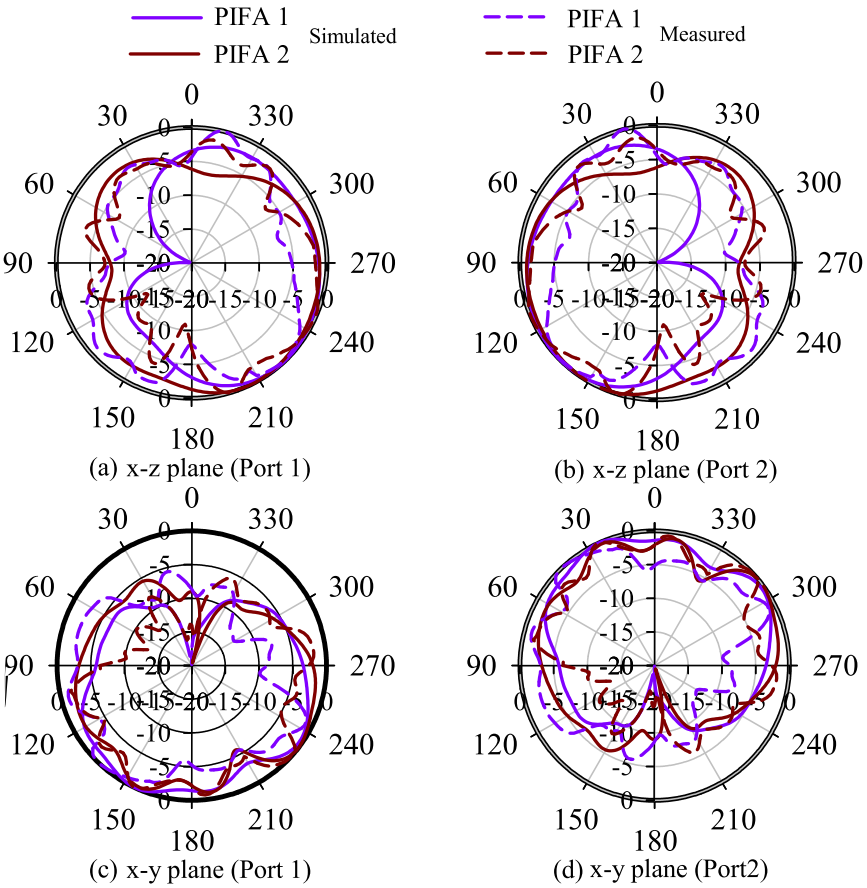

FIGURE 9. Comparative polar radiation pattern results of PIFA element 1 and 2 observed at 4.5 GHz. The results are depicted in xz-plane for (a) port 1 and (b) port 2 and illustrated in xy-plane for (c) port 1 and (d) port 2.

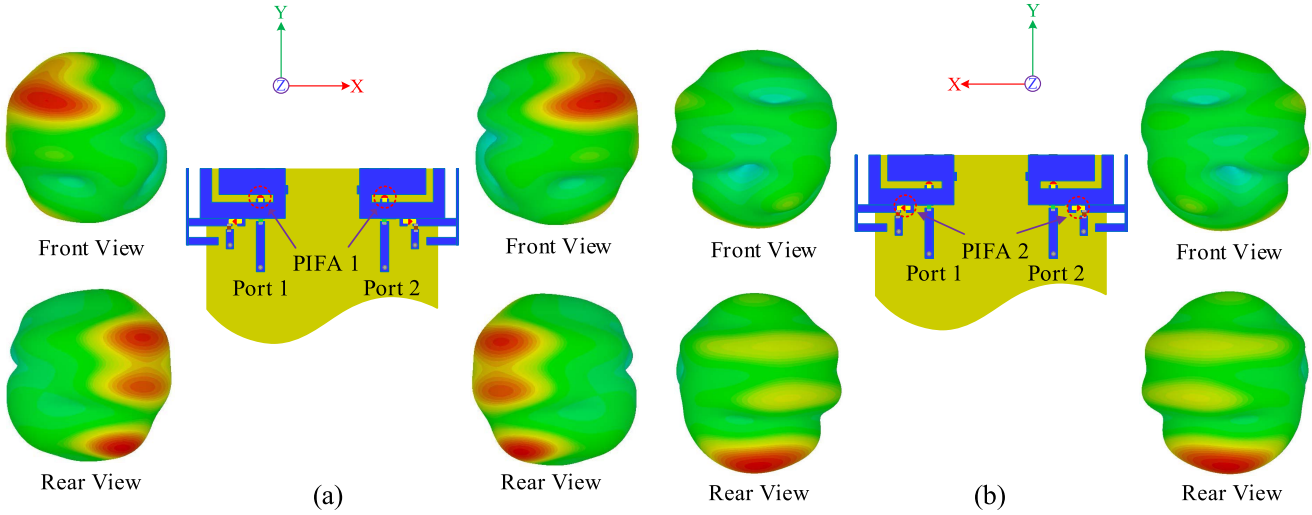

FIGURE 10. The simulated 3-D radiation pattern results obtained at 4.5 GHz when the identical PIFA elements from port 1 and 2 are activated (a) PIFA element 1 (b) PIFA element 2.

In comparison to previously reported MIMO antennas, our proposed antenna is capable of multiband operation across a wide range of cellular bands, including 5G-NR bands, despite being constructed on a small sized substrate with a compact antenna structure. Furthermore, it has achieved good calculated total efficiency, resulting in a low ECC value and high channel capacity. The comparison study shows that achieving all of these antenna characteristics simultaneously for mobile phone applications is considered a challenging factor in previous reported MIMO antenna designs due to space constraints and complexity. The most critical part in designing this type of antenna is the reconfiguration of

TABLE 3. The details of radiation pattern reconfiguration observed at 4.5 GHz.

Resonant Frequency (GHz)	Ports	Activated PIFA Elements	Main Lobe Direction (deg) (xz-plane)	Angular Width (3 dB) (xz - plane)	Main Lobe Mag (dB)	Main Lobe Direction (deg) (xy-plane)	Angular Width (3 dB) (xy - plane)	Main Lobe Mag (dB)
4.5	Port 1	PIFA 1	223	174.1	2.12	155	96.1	2.31
		PIFA 2	207	176.1	0.506	232	62.1	1.58
	Port 2	PIFA 1	137	174.1	2.12	25	96.1	2.31
		PIFA 2	153	176.1	0.506	308	62.1	1.58

TABLE 4. Comparison of the proposed antenna against related literatures.

Reference	Antenna type	MIMO element	Overall size	Single Antenna volume (λ_0)	Bandwidth (S11/S22 < -6 dB)	Covered Cellular Bands	Calculated Efficiency (%)	ECC	Calculated Channel capacity (bit/s/Hz)
[19]	Dual band	8 x 8	150 x 70	0.22 x 0.08	3300~4200, 5000	5G-NR	53 ~ 79.5	< 0.15	8 x 8: 40
[15]	FRn	2 x 2 4 x 4	160 x 85	0.12 x 0.008 0.13 x 0.008	2 x 2: 824 ~ 960 4 x 4: 1710 ~ 2690	2 x 2: GSM 4 x 4: DCS/PCS, UMTS & LTE	2 x 2: 37~54 4 x 4: 55~73	< 0.3 < 0.15	2 x 2: 10 4 x 4: 20
[16]	RPRn	8 x 8	-	0.33 x 0.036 x 0.167	4500~5500	5 GHz WLAN	-	< 0.05	-
[17]	FRn	2.x2	145 x 72	0.09 x 0.054	824~960, 1710~2690	GSM, UMTS, LTE	43 ~ 72	< 0.34	9 ~ 10
[18]	FRn	2 x 2	100 x 63	0.05 x 0.11	800~980, 1650~2220	LTE	-	< 0.3	-
Proposed	Multiband, FRn and RPRn	2 x 2	120 x 60	PIFA 1: 0.06 x 0.04 x 0.021 PIFA 2: 0.12 x 0.05 x 0.05	PIFA 1: 800 ~ 1060, 3330 ~ 5660 PIFA 2: 1660 ~ 2170, 2440 ~ 2660, 3670 ~ 5670	T-GSM, E- GSM, R-GSM, UMTS, LTE, 5G-NR	PIFA 1: 46.2 ~ 74.5 PIFA 2: 55.2 ~ 65	PIFA 1: < 0.26 PIFA 2: < 0.08	PIFA 1: 9.5 ~ 10.5 PIFA 2: 9.72 ~ 10.23

Legend: FRn: Frequency Reconfiguration; RPRn: Radiation Pattern Reconfiguration

radiation pattern and frequency as it involves RF switches and lumped components. Nevertheless, with proper design and space utilization technique, the proposed compact antenna successfully performs frequency reconfiguration together with radiation pattern reconfiguration, besides being multiband.

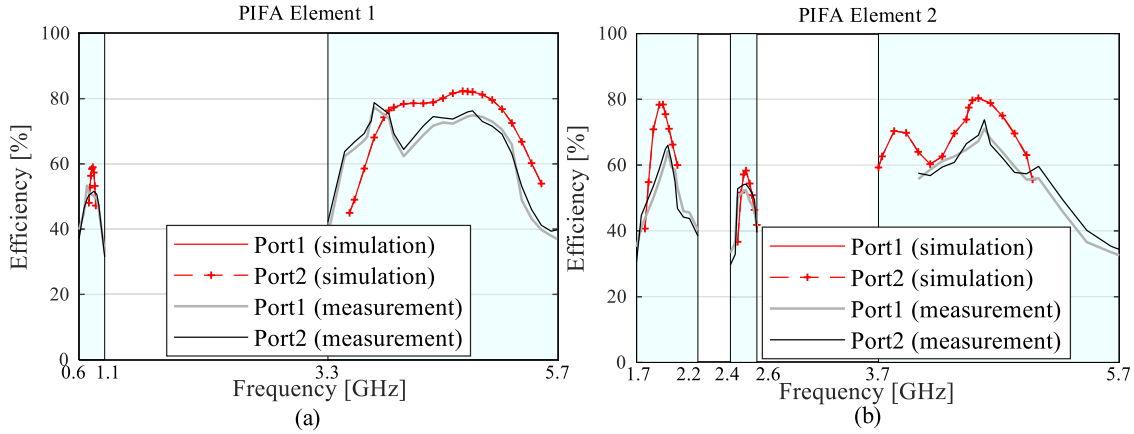

FIGURE 11. Simulated and measured total efficiency in free space for: (a) PIFA element 1 and (b) PIFA element 2.

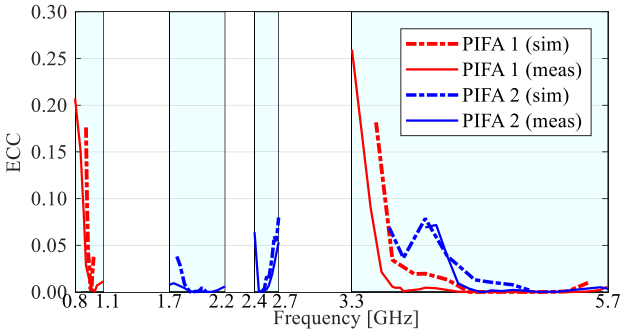

FIGURE 12. The simulated and measured ECC between port 1 and port 2 of PIFA element 1 and PIFA element 2.

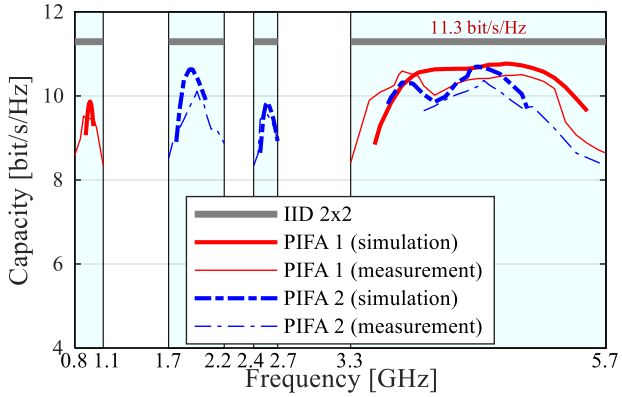

FIGURE 13. The simulated and calculated ergodic channel capacity results of the PIFA element 1 and PIFA element 2 in free space over the entire frequency band.

IV. CONCLUSION

In this letter, a multiband two port MIMO antenna with compound beam and frequency reconfiguration for sub-6 GHz 5G mobile terminal applications is investigated. It is able to operate within the GSM, UMTS, LTE and 5G-NR cellular bands with $S_{11} < -6$dB, ranging from 0.8 GHz to 6 GHz. Furthermore, beam and frequency reconfigurations are achieved using PIN diodes switching between PIFA element 1 and 2. Besides that, the transmission coefficient and ECC of less than −10 dB and 0.26, respectively, indicates its satisfactory isolation and diversity performance. Its compact size with total efficiency of more than 46.3% and channel capacity of 9.5 bit/s/Hz makes it suitable for application in 5G mobile terminals.

REFERENCES

[1] R. Hussain, A. T. Alreshaid, S. K. Podilchak, and M. S. Sharawi, "Compact 4G MIMO antenna integrated with a 5G array for current and future mobile handsets," *IET Microw., Antennas Propag.*, vol. 11, no. 2, pp. 271–279, Jan. 2017.

[2] S. Zhang, K. Zhao, Z. Ying, and S. He, "Investigation of diagonal antenna-chassis mode in mobile terminal LTE MIMO antennas for bandwidth enhancement," *IEEE Antennas Propag. Mag.*, vol. 57, no. 2, pp. 217–228, Apr. 2015.

[3] H. Hu, H. Gao, Z. Li, and Y. Zhu, "A sub 6 GHz massive MIMO system for 5G new radio," in *Proc. IEEE 85th Veh. Technol. Conf. (VTC Spring)*, Jun. 2017, pp. 1–5.

[4] A. Al-Dulaimi, S. Al-Rubaye, Q. Ni, and E. Sousa, "5G communications race: Pursuit of more capacity triggers LTE in unlicensed band," *IEEE Veh. Technol. Mag.*, vol. 10, no. 1, pp. 43–51, Mar. 2015.

[5] S. Mudda, G. Km, and M. Mallikarjun, "Wide-band frequency tunable antenna for 4G, 5G/sub 6 GHz portable devices and MIMO applications," *Prog. Electromagn. Res. C*, vol. 118, pp. 25–41, 2022.

[6] Y.-L. Ban, C. Li, C.-Y.-D. Sim, G. Wu, and K.-L. Wong, "4G/5G multiple antennas for future multi-mode smartphone applications," *IEEE Access*, vol. 4, pp. 2981–2988, 2016.

[7] Y. Li, C.-Y.-D. Sim, Y. Luo, and G. Yang, "Multiband 10-antenna array for sub-6 GHz MIMO applications in 5-G smartphones," *IEEE Access*, vol. 6, pp. 28041–28053, 2018.

[8] J. Costantine, Y. Tawk, S. E. Barbin, and C. G. Christodoulou, "Reconfigurable antennas: Design and applications," *Proc. IEEE*, vol. 103, no. 3, pp. 424–437, Mar. 2015.

[9] S. Padmanathan, A. A. Al-Hadi, P. J. Soh, and M. F. Jamlos, "Reconfigurable antennas for MIMO applications: An overview," in *Proc. IEEE Student Conf. Res. Develop. (SCOReD)*, Dec. 2015, pp. 193–197.

[10] W.-W. Lee and B. Jang, "A tunable MIMO antenna with dual-port structure for mobile phones," *IEEE Access*, vol. 7, pp. 34113–34120, 2019.

[11] C. Rhee, Y. Kim, T. Park, S. Kwoun, and B. Mun, "Pattern-reconfigurable MIMO antenna for high isolation and low correlation," *IEEE Antennas Wireless Propag. Lett.*, vol. 13, pp. 1373–1376, 2014.

[12] S. Riaz and X. Zhao, "An 8-element frequency-agile MIMO communication antenna system for CR front-end applications," *Prog. Electromagn. Res. C*, vol. 84, pp. 75–85, 2018.

[13] K. Diallo, A. Diallo, I. Dioum, S. Ouya, and J. M. Ribero, "Design of a dual-band antenna system for LTE-M and LTE-MIMO by exploiting the characteristic mode theory," *Prog. Electromagn. Res. M*, vol. 93, pp. 11–21, 2020.

[14] J. Choi, W. Hwang, C. You, B. Jung, and W. Hong, "Four-element reconfigurable coupled loop MIMO antenna featuring LTE full-band operation for metallic-rimmed smartphone," *IEEE Trans. Antennas Propag.*, vol. 67, no. 1, pp. 99–107, Jan. 2019.

[15] Y.-H. Zhang, S.-R. Yang, Y.-L. Ban, Y.-F. Qiang, J. Guo, and Z.-F. Yu, "Four-feed reconfigurable MIMO antenna for metal-frame smartphone applications," *IET Microw., Antennas Propag.*, vol. 12, no. 9, pp. 1477–1482, Jul. 2018.
[16] N. H. Chamok, M. H. Yılmaz, A. Arslan, and M. Ali, "High-gain pattern reconfigurable MIMO antenna array for wireless handheld terminals," *IEEE Trans. Antennas Propag.*, vol. 64, no. 10, pp. 4306–4315, Oct. 2016.
[17] Z.-Q. Xu, Y. Sun, Q.-Q. Zhou, Y.-L. Ban, Y.-X. Li, and S. S. Ang, "Reconfigurable MIMO antenna for integrated-metal-rimmed smartphone applications," *IEEE Access*, vol. 5, pp. 21223–21228, 2017.
[18] G. Shruthi and C. Y. Kumar, "Dual-band frequency-reconfigurable MIMO PIFA for LTE applications in mobile hand-held devices," *IET Microw., Antennas Propag.*, vol. 14, no. 5, pp. 419–427, 2020.
[19] L. Cui, J. Guo, Y. Liu, and C.-Y.-D. Sim, "An 8-element dual-band MIMO antenna with decoupling stub for 5G smartphone applications," *IEEE Antennas Wireless Propag. Lett.*, vol. 18, no. 10, pp. 2095–2099, Oct. 2019.
[20] H.-D. Chen, Y.-C. Tsai, C.-Y.-D. Sim, and C. Kuo, "Broadband eight-antenna array design for sub-6 GHz 5G NR bands metal-frame smartphone applications," *IEEE Antennas Wireless Propag. Lett.*, vol. 19, no. 7, pp. 1078–1082, Jul. 2020.
[21] D. Serghiou, M. Khalily, V. Singh, A. Araghi, and R. Tafazolli, "Sub-6 GHz dual-band 8×8 MIMO antenna for 5G smartphones," *IEEE Antennas Wireless Propag. Lett.*, vol. 19, no. 9, pp. 1546–1550, Sep. 2020.
[22] A. M. Elshirkasi, A. A. Al-Hadi, P. J. Soh, M. F. Mansor, R. Khan, X. Chen, and P. Akkaraekthalin, "Performance study of a MIMO mobile terminal with upto 18 elements operating in the sub-6 GHz 5G band with user hand," *IEEE Access*, vol. 8, pp. 28164–28177, 2020.

SURENTIRAN PADMANATHAN (Member, IEEE) received the B.Eng. degree in communication engineering, in 2014. He is currently pursuing the Doctor of Philosophy (Ph.D.) degree in communication engineering with the Faculty of Electronic Engineering Technology, Universiti Malaysia Perlis (UniMAP). His research interests include reconfigurable antenna, mobile terminal antenna, MIMO antenna, MIMO performance evaluation, and wireless propagation.

AZREMI ABDULLAH AL-HADI (Senior Member, IEEE) received the Master of Science degree in communication engineering from Birmingham University, U.K., in 2004, and the Doctor of Science degree in technology from Aalto University, Finland, in 2013.

He is currently working as an Associate Professor and holds position as the Dean of the Faculty of Electronic Engineering Technology, Universiti Malaysia Perlis (UniMAP). He has been with the university, since 2002. His current research interests include design and performance evaluation of multi-element antennas, mobile terminal antennas and their user interactions, and wireless propagation.

Dr. Abdullah Al-Hadi was a recipient of the Best Student Paper Award presented at the 5th Loughborough Antennas and Propagation Conference (LAPC 2009), the CST University Publication Award, in 2011, and the Excellence and best paper awards from IEEE Malaysia AP/MTT/EMC Joint Chapter, in 2018, 2019, and 2020. He is the Chartered Engineer of the Institution of Engineering and Technology (IET), U.K., the Professional Technologist of the Malaysia Board of Technologist (MBOT), Malaysia, and a member of the Board of Engineers Malaysia (BEM), Malaysia. During his appointment as the Vice Chair of the IEEE Malaysia AP/MTT/EMC Joint Chapter, the Chapter has won the 2020 Outstanding Chapter Award by the IEEE Antennas and Propagation Society. He is active in volunteering work with IEEE Malaysia Section, acting as the Chair of the IEEE Malaysia Antenna Propagation/Microwave Theory Techniques/Electromagnetic Compatibility (AP/MTT/EMC) Joint Chapter, and the Past Counselor for the IEEE UniMAP Student Branch.

AHMED MOHAMED ELSHIRKASI received the M.Sc. degree in communication engineering from International Islamic University Malaysia (IIUM), in 2015, and the Ph.D. degree from Universiti Malaysia Perlis (UniMAP), in 2021. His current research interests include the performance evaluation of MIMO antennas, mobile terminal antennas and their user interactions, and wireless propagation.

SAMIR SALEM AL-BAWRI (Member, IEEE) received the Master of Science degree in wireless communication engineering from Yarmouk University, Jordan, in 2009, and the Doctor of Philosophy degree in communication engineering from Universiti Malaysia Perlis (UniMAP), Malaysia, in 2018. He has worked as a Lecturer with the Faculty of Engineering and Petroleum, Hadhramout University (HU), Yemen, from December 2009 to August 2014. He worked as a Graduate Research Assistance with UniMAP, from 2015 to 2018. He has worked as a Postdoctoral Researcher Fellow with Multimedia University (MMU), Cyberjaya, Malaysia, for one year. He is currently affiliated as a Senior Lecturer/a Research Fellow with the Center for Space Science, Institute of Climate Change, Universiti Kebangsaan Malaysia (UKM). He has authored or coauthored over (25) ISI and SCOPUS published journal; (22) conference proceeding on various topics related to antennas, microwaves, and electromagnetic radiation analysis with one inventory patent. His research interests include design and evaluation of multi-element antennas, metamaterials, electromagnetic radiation analysis, localization estimation techniques, and wireless propagation. He was a recipient of the Gold Medal Award at the Breakthrough Invention, Innovation & Design Exhibition Biide2019—UiTM. He was also a recipient of the Gold Medal Award at the Breakthrough Invention, Innovation & Design Exhibition Biide2019, UiTM, and Research Innovation Commercialization and Entrepreneurship Showcase (RICES) 2021, MMU. He currently serves as the Editor Manager for *International Journal of Multidisciplinary Sciences and Advanced Technology* (IJMSAT).

MOHAMMAD TARIQUL ISLAM (Senior Member, IEEE) is currently a Professor with the Department of Electrical, Electronic and Systems Engineering, Universiti Kebangsaan Malaysia (UKM), and a Visiting Professor with the Kyushu Institute of Technology, Japan. He is the author and coauthor of about 600 research journal articles, nearly 250 conference papers, and a few book chapters on various topics related to antennas, metamaterials, and microwave imaging with 23 inventory patents filed. Thus far, his publications have been cited 8150 times and his H-index is 42 (Source: Scopus). His Google scholar citation is 14,000 and H-index is 51. He was a recipient of more than 40 research grants from the Malaysian Ministry of Science, Technology and Innovation, Ministry of Education, UKM Research Grant, International Research Grants from Japan, Saudi Arabia, and Kuwait. He has developed the Antenna Measurement Laboratory, which includes antenna design and measurement facility till 40 GHz. He has supervised about 50 Ph.D. theses, 30 M.Sc. theses, and has mentored more than ten postdoctoral researchers and a visiting scholars. His research interests include communication antenna design, metamaterial, satellite antennas, and microwave imaging. He was served as an Executive Committee Member for IEEE AP/MTT/EMC Malaysia Chapter, from 2019 to 2020, the Chartered Professional Engineer (C.Eng.), a fellow of IET, U.K., and a Senior Member of IEICE, Japan. He received several international gold medal awards, a Best Invention in Telecommunication Award for his Research and Innovation, and Best Researcher Awards at UKM. He was a recipient of 2018, 2019, and 2020 IEEE AP/MTT/EMC Malaysia Chapter, Excellent Award. He was also a recipient of Publication

Award from Malaysian Space Agency, in several years. He also won the Best Innovation Award and the Best Research Group in ICT niche by UKM, in different years. He was an Associate Editor of *IET Electronics Letter*. He also serves as the Guest Editor for *Sensors* journal, and an Associate Editor for IEEE Access.

THENNARASAN SABAPATHY (Member, IEEE) received the B.Eng. degree in electrical telecommunication engineering from Universiti Teknologi Malaysia, in 2007, the M.Sc. (Eng.) degree from Multimedia University, Malaysia, in 2011, and the Ph.D. degree in communication engineering from University Malaysia Perlis, in 2014. In 2007, he worked as a Test Development Engineer at Flextronics, working on the hardware and software test solutions for the mobile phone manufacturing. Then, he joined Multimedia University as a Research Officer, from 2008 to 2010, while pursuing his M.Sc. (Eng.) degree. From 2012 to 2014, he was a Research Fellow with University Malaysia Perlis, during his Ph.D. degree, where he is currently an Associate Professor with the Faculty of Electronic Engineering Technology. His current research interests include antenna and propagation, millimeter-wave wireless communications, and metamaterial/metasurface.

MUZAMMIL JUSOH (Senior Member, IEEE) received the bachelor's degree in electrical-electronic and telecommunication engineering and the M.Sc. degree in electronic telecommunication engineering from Universiti Teknologi Malaysia (UTM), in 2006 and 2010, respectively, and the Ph.D. degree in communication engineering from Universiti Malaysia Perlis (UniMAP), in 2013. He is currently an Associate Professor. He is also a Research Fellow of the Advanced Communication Engineering (ACE) Centre of Excellence (CoE), UniMAP. His experience as a RF Engineer and a Microwave Engineer with Telekom Malaysia Berhad (TM) Company, from 2006 to 2009, performed as the Team Leader of the Specialized Network Services (SNS) Department-based in TM Senai Johor. He is involved in preventive and corrective maintenance of ILS, NDB, DVOR, repeaters, microwave systems, VHF, and UHF. He has Score H-index of 19 (SCOPUS index) and leading few grants as a main/a co-researcher under the Ministry of Higher Education Malaysia, Industrial Grants, and Internal Grant from UniMAP worth in total USD430k. He is currently supervising/graduate more than 20 postgraduate students (M.Sc. and Ph.D.). He has published over 240 articles in journals and proceedings, including IEEE Access, *Sensors* (MDPI), *Materials*, IEEE Antenna and Wireless Propagation Letter (AWPL), *Microwave and Optical Technology Letter* (MOTL), *International Journal on Antenna and Propagation* (IJAP), and *Progress in Electromagnetics Research* (PIER) with more than 100 conference papers. His research interests include antenna design, reconfigurable beam steering antennas, RFID, MIMO, UWB, wireless on-body communications, and RF and microwave communication systems. Besides, he has been a member of the technical program committees of several IEEE conferences and a technical reviewer for several IEEE and other conferences. Moreover, he is a member of the IET (MIET), the Antenna and Propagation Society (AP/MTT/EMC) Malaysia Chapter, and IEEE RFID Council.

PRAYOOT AKKARAEKTHALIN (Senior Member, IEEE) received the B.Eng. and M.Eng. degrees in electrical engineering from the King Mongkut's University of Technology North Bangkok (KMUTNB), Bangkok, Thailand, in 1986 and 1990, respectively, and the Ph.D. degree from the University of Delaware, Newark, DE, USA, in 1998. From 1986 to 1988, he was a Research and Development Engineer with Microtek Company Ltd., Thailand. In 1988, he joined the Department of Electrical Engineering, KMUTNB. From 2014 to 2020, he was the Leader of TRF Senior Research Scholar Project. He is currently the Head of the Innovative Sensor Technology Research Group, KMUTNB. He has authored or coauthored over 80 international journals, more than 250 conference papers, and six books/book chapters. His current research interests include RF/microwave circuits, wideband and multiband antennas, telecommunications, and sensor systems. He is a member of the IEICE Japan, ECTI, and EEAAT Associations Thailand. He was the Editor-in-Chief of the *ECTI Transactions*, from 2011 to 2013. He was the Chairman of the IEEE MTT/AP/ED Thailand Joint Chapter, from 2007 to 2010, and the Vice President and the President of the ECTI Association, Thailand, from 2012 to 2013, and from 2014 to 2015, respectively.

PING JACK SOH (Senior Member, IEEE) was born in Sabah, Malaysia. He received the bachelor's and master's degrees from Universiti Teknologi Malaysia and the Ph.D. degree from KU Leuven, Belgium.

He started his career as a Test Engineer at Venture Corporation, and a Research and Development Engineer at Motorola Solutions Malaysia. Then, he was a Lecturer with Universiti Malaysia Perlis (UniMAP) before moving to KU Leuven as a Research Assistant and a Postdoctoral Research Fellow. Since 2014, he has been a Research Affiliate with the ESAT-WAVECORE Research Division. He returned to UniMAP as a Senior Lecturer and an Associate Professor, until 2021, before moving to Finland. Within UniMAP, he was formerly the Deputy Director of the Centre for Industrial Collaboration (2007–2009), the Deputy Dean of the University's Research Management and Innovation Center (RMIC) (2014–2017), and the Head of the Advanced Communication Engineering (ACE) Research Centre, in 2020. He is currently an Associate Professor with the Centre for Wireless Communications (CWC), University of Oulu, Finland. He is also the Coordinator for the ''Devices and Circuit Technology'' strategic research area within the 6G Flaghip program. He has published more than 300 articles in journals and international conference proceedings, besides four book chapters. His research interests include antennas and their applications in wearables/body area communication, metasurfaces and reflectors, 5G/6G communications, compact satellites, EM safety and absorption, and wireless techniques for healthcare. He is also an Associate Editor of the *International Journal of Numerical Modelling: Electronic Networks, Devices and Fields* (Wiley).

Dr. Soh was a recipient of the URSI Young Scientist Award, in 2015, the IEEE MTT-S Graduate Fellowship for Medical Applications, in 2013 and the IEEE AP-S Doctoral Research Award, in 2012. He was also the Second Place Winner of the IEEE President's Change the World Competition, in 2013. Two of his (co)authored journals were awarded the CST University Publication Award, in 2012 and 2011. He is a Chartered Engineer registered with U.K. Engineering Council, and a member of the IET and URSI. He also volunteers in the IEEE MTT-S Education Committee.